THE JOURNAL OF BIOLOGICAL CHEMISTRY VOL. 281, NO. 45, pp. 33892–33899, November 10, 2006

Inhibition of Fructose-1,6-bisphosphatase by Aminoimidazole Carboxamide Ribotide Prevents Growth of *Salmonella enterica purH* Mutants on Glycerol*

Received for publication, May 9, 2006, and in revised form, September 20, 2006 Published, JBC Papers in Press, September 20, 2006, DOI 10.1074/jbc.M604429200

Michael J. Dougherty[1], **Jeffrey M. Boyd, and Diana M. Downs**[2]

From the Department of Bacteriology, University of Wisconsin, Madison, Wisconsin 53706

The enzyme fructose-1,6-bisphosphatase (FBP) is key regulatory point in gluconeogenesis. Mutants of *Salmonella enterica* lacking *purH* accumulate 5-amino-4-imidazole carboxamide ribotide (AICAR) and are unable to utilize glycerol as sole carbon and energy sources. The work described here demonstrates this lack of growth is due to inhibition of FBP by AICAR. Mutant alleles of *fbp* that restore growth on glycerol encode proteins resistant to inhibition by AICAR and the allosteric regulator AMP. This is the first report of biochemical characterization of substitutions causing AMP resistance in a bacterial FBP. Inhibition of FBP activity by AICAR occurs at physiologically relevant concentrations and may represent a form of regulation of gluconeogenic flux in *Salmonella enterica*.

An efficient cellular metabolism that can adapt to changing environmental conditions requires the integration of many biochemical pathways. Subtle interactions that exist between pathways in the metabolic network are in general not well understood. One level of these interactions involves metabolites common to multiple pathways. Cellular metabolites can impact physiology through roles in transcriptional regulation, translational regulation, or by mediating allosteric effects on key enzymes. One such central metabolite with regulatory capabilities is 5-amino-4-imidazole carboxamide ribotide (AICAR).[3]

AICAR is a purine nucleotide biosynthetic intermediate and the substrate for AICAR transformylase/IMP cyclohydrolase, encoded by the *purH* gene in *Salmonella enterica*. AICAR is also generated as a byproduct of histidine biosynthesis, released by the enzyme imidazole glycerol-phosphate synthase (Fig. 1*A*). AICAR has been shown to impact different metabolic pathways in diverse organisms. Bochner and Ames (1) proposed that 5-amino-4-imidazole carboxamide riboside 5′-triphosphate formed from the accumulation of AICAR is an alarmone for C1-folate deficiency in *S. enterica*, although this conclusion, in its simplest form, was not supported by subsequent work (2). AICAR has been shown to be a negative effector of cytochrome terminal oxidase cbb_3 production in *Rhizobium etli* (3) and was recently shown to affect regulation of purine biosynthesis genes in *Saccharomyces cerevisiae* (4). Previous work from our laboratory demonstrated that AICAR accumulation inhibits the conversion of aminoimidazole ribotide to 4-amino-5-hydroxymethyl-2-methyl pyrimidine phosphate in the biosynthesis of thiamine pyrophosphate in *S. enterica* (5).

In mammalian systems, AICAR has been shown to activate AMP-activated protein kinase (6), which plays a critical role in energy balance and the response to metabolic stress (7). Through activation of AMP-activated protein kinase, AICAR inhibits proliferation of several types of cancer cells (8, 9). Furthermore, AICAR has been shown to inhibit gluconeogenesis in mammals due to inhibition of fructose-1,6-bisphosphatase (10, 11).

Fructose-1,6-bisphosphatase (D-fructose-1,6-bisphosphate 1-phosphohydrolase, EC 3.1.3.11; FBP) catalyzes the hydrolysis of fructose 1,6-bisphosphate (Fru-1,6-P) to fructose 6-phosphate and inorganic phosphate (12). FBP is important for the regulation of flux between glycolysis and gluconeogenesis (Fig. 1*B*); as the enzyme is inhibited by AMP and fructose 2,6-bisphosphate (Fru-2,6-P) (13). Fru-2,6-P is a competitive inhibitor with respect to the substrate Fru-1,6-P, which binds at the active site (14, 15), whereas AMP binds to an allosteric site (16, 17), which causes a structural transition from the active R state of the enzyme to the inactive T state (18). FBP from mammalian sources has been extensively studied at the biochemical level. In *Escherichia coli*, FBP activity is required for growth on glycerol, succinate, or acetate as sole carbon and energy source (19). *E. coli* FBP has been shown to be activated by Mg^{2+} and inhibited by AMP and Fru-2,6-P, similar to the mammalian enzymes, although Mg^{2+} activation and AMP inhibition did not display cooperativity, as in the mammalian enzymes (20). The physiological relevance of Fru-2,6-P inhibition of *E. coli* FBP is not clear; Fru-2,6-P inhibition is not synergistic with AMP inhibition as in mammalian systems (20, 21), and to date Fru-2,6-P has not been found in bacterial cells (22). Phosphoenolpyruvate has been shown to relieve AMP inhibition of *E. coli* FBP (21, 23). Recently, the crystal structure of *E. coli* FBP was reported;

* This work was supported in part by competitive Grant GM47296 from the National Institutes of Health and funds from a 21st Century Scientist Scholars Award from the J. S. McDonnell Foundation. The costs of publication of this article were defrayed in part by the payment of page charges. This article must therefore be hereby marked "*advertisement*" in accordance with 18 U.S.C. Section 1734 solely to indicate this fact.

[1] Supported by Biotechnology Traineeship Grant T32 GM08349 from the National Institutes of Health, a Louis and Elsa Thomsen Wisconsin Distinguished Fellowship Award, and the William H. Peterson Predoctoral Fellowship from the Department of Bacteriology. Present address: Div. of Chemistry and Chemical Engineering, 210-41, California Institute of Technology, Pasadena, CA 91125.

[2] To whom correspondence should be addressed: 420 Henry Mall, Madison, WI 53706. Tel.: 608-265-4630; Fax: 608-262-9865; E-mail: downs@bact.wisc.edu.

[3] The abbreviations used are: AICAR, 5-amino-4-imidazole carboxamide ribotide; FBP, fructose-1,6-bisphosphatase; Fru-1,6-P, fructose 1,6-bisphosphate; Fru-2,6-P, fructose 2,6-bisphosphate.

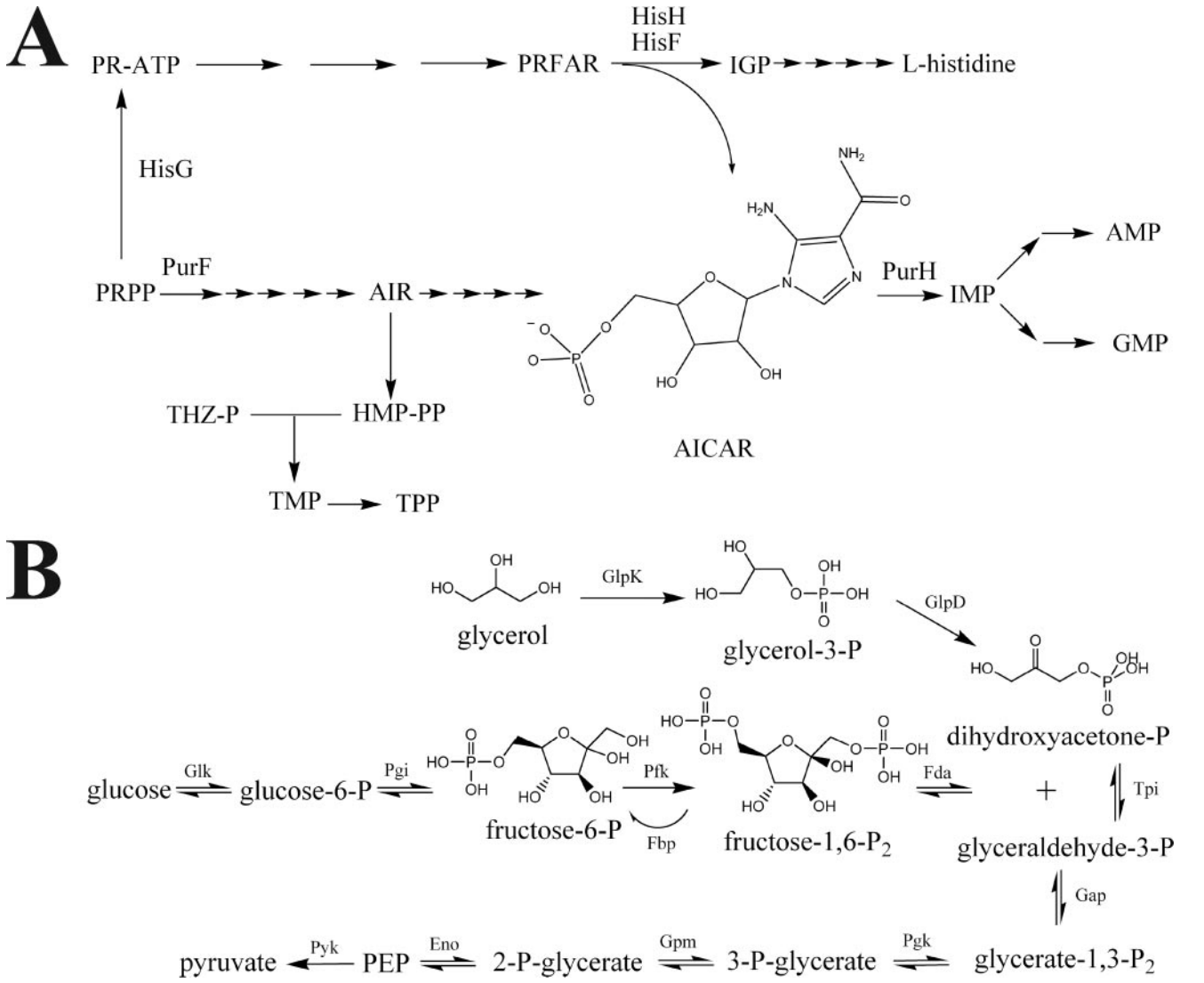

FIGURE 1. *A*, the purine and histidine biosynthetic pathways in *S. enterica*. *B*, glycolysis, gluconeogenesis, and the glycerol utilization pathways in *S. enterica*. Gene products catalyzing the reaction are indicated *above* the relevant steps.

these authors also demonstrated activation of FBP by phosphoenolpyruvate and postulated a novel allosteric binding site for this compound (24).

The studies described here demonstrate that *purH* mutants of *S. enterica* are unable to use glycerol or other gluconeogenic carbon sources in the absence of exogenous histidine. Results show that this growth phenotype is due to inhibition of FBP by the accumulation of AICAR. AICAR-resistant alleles of *fbp* were isolated and the mutant proteins were purified and characterized *in vitro*. FBP is inhibited by AICAR at physiologically relevant concentrations and thus this interaction may represent a form of regulation relevant under some growth conditions, such as folate stress.

EXPERIMENTAL PROCEDURES

Bacterial Strains, Media, and Chemicals

All strains used in this study are derivatives of *S. enterica* LT2 and are listed with their genotypes in Table 1. The *purH355* allele contains a thymidine inserted at position 716, resulting in a frameshift and generating a truncated PurH protein of 266 amino acids. MudJ refers to the Mu*d*1734 insertion element (25) and Tn*10d*(Tc) refers to the transposition-defective mini-Tn*10* described by Way *et al.* (26). No-carbon E medium supplemented with 1 mM $MgSO_4$ (27, 28) and glucose (11 mM) or glycerol (22 mM) was used as a minimal medium. Difco nutrient broth (8 g/liters) with NaCl (5 g/liters) and Luria-Bertani broth were used as rich media. Difco BiTek agar was added (15 g/liter) for solid medium. When present in the media, supplements were provided at the following final concentrations: thiamine, 10 or 100 nM; adenine, 0.4 mM; histidine, 74 μM. When needed, antibiotics were added to the following concentrations in rich/minimal media: tetracycline, 20/10 μg/ml; kanamycin, 50/125 μg/ml; chloramphenicol, 20/4 μg/ml; and ampicillin, 50/15 μg/ml. Restriction enzymes and DNA ligase were purchased from Promega (Madison, WI). Cloned *Pfu* DNA polymerase was purchased from Stratagene (La Jolla, CA).

Genetic Methods

Phenotypic Analysis—Nutritional requirements were assessed on solid medium with soft agar overlays and by quantification of

TABLE 1

Strains and plasmids

All strains and plasmids were generated for this study or are part of laboratory stock unless indicated.

Strain	Genotype
DM2	*purH355*
DM7596	*zja8039*::Tn*10*d(Tc) *purH355*
DM7597	*zja8039*::Tn*10*d(Tc)
DM7833	*fbp-21*::MudJ
DM8807	*zja8039*::Tn*10*d(Tc) *purH355 stm4417-8*::Tn*10*d(Cm) *fbp-22*
DM8808	*zja8039*::Tn*10*d(Tc) *purH355 stm4417-8*::Tn*10*d(Cm)
DM8809	*zja8039*::Tn*10*d(Tc) *purH355 stm4417-8*::Tn*10*d(Cm) *fbp-23*
DM8810	*zja8039*::Tn*10*d(Tc) *purH355 stm4417-8*::Tn*10*d(Cm)
DM8811	*zja8039*::Tn*10*d(Tc) *purH355 stm4417-8*::Tn*10*d(Cm) *fbp-24*
DM8812	*zja8039*::Tn*10*d(Tc) *purH355 stm4417-8*::Tn*10*d(Cm)
DM9296	*aadA*::*araC-*P_{BAD}*-*T_7 *fbp-21*::MudJ
DM9297	*aadA*::*araC-*P_{BAD}*-*T_7 *fbp-21*::MudJ/pLysS
DM9299	*aadA*::*araC-*P_{BAD}*-*T_7 *fbp-21*::MudJ/pLysS/pMD84
DM9230	*aadA*::*araC-*P_{BAD}*-*T_7 *fbp-21*::MudJ/pLysS/pMD103
DM9231	*aadA*::*araC-*P_{BAD}*-*T_7 *fbp-21*::MudJ/pLysS/pMD104
DM9232	*aadA*::*araC-*P_{BAD}*-*T_7 *fbp-21*::MudJ/pLysS/pMD105
SB300A#1	*aadA*::*araC-*P_{BAD}*-*T_7[a]
Plasmids	Vector and insert
pMD51	pSU19 (Cm^R)[b]; *fbp*
pMD56	pSU19 (Cm^R); *fbp-22* (T19I)
pMD57	pSU19 (Cm^R); *fbp-23* (G20D)
pMD58	pSU19 (Cm^R); *fbp-24* (T23I)
pMD84	pET20 b(+)(Amp^R)[c]; *fbp*
pMD103	pET20 b(+)(Amp^R); *fbp-22* (T19I)
pMD104	pET20 b(+)(Amp^R); *fbp-23* (G20D)
pMD105	pET20 b(+)(Amp^R); *fbp-24* (T23I)
pLysS	pACYC184 (Cm^R)[d]; T7 gene 3.5[e]

[a] SB300A#1 was obtained from J. McKinney (51).
[b] Construction of pSU19 was described previously (52).
[c] Plasmid pET20 b(+) was purchased from Novagen (Madison, WI).
[d] Construction of pACYC184 was described previously (53).
[e] Described by Studier (54).

growth in liquid media. Protocols for each have been previously described (29, 30).

Transduction Methods—The high-frequency generalized transducing mutant version of bacteriophage P22 (HT105/1 *int-201*) was used in all transductions (31, 32). The methods for transduction and purification of transductants have been previously described (33).

Isolation of Linked Insertions—Transposons (Tn*10d*(Tc)) genetically linked to the mutation allowing utilization of glycerol as sole carbon source in a *purH* mutant were isolated by standard genetic techniques (34). The chromosomal location of each insertion was determined by sequencing using a PCR-based protocol (35, 36). A DNA product was amplified with degenerate primers and primers derived from the Tn*10d*(Tc) insertion sequence as described and sequenced at the University of Wisconsin Biotechnology DNA Sequence Facility.

Molecular Biology Techniques

The *fbp* gene was amplified from wild-type and mutant strains using genomic DNA as a template and the forward primer, 5′-TACTTTGCTGGCGCGATTCACCTG-3′, and the reverse primer, 5′-TGTTTTCGTTTCCGCCTCATCTGG-3′. The resulting PCR products were purified and ligated into SmaI-cut pSU19. Plasmids were transformed into *E. coli* strain DH5α and screened for vectors containing inserts. The identity of the resulting plasmids was confirmed by sequencing. Plasmids for expression of His-tagged FBP were constructed as described above using plasmid DNA as the template and the forward primer 5′-GCAGGGAAAGTCATATGAAAACG-3′ and the reverse primer 5′-CTCGAGCGCGTCCGGGTATTCGCGGATAAA-3′ (engineered restriction sites underlined). These PCR products were ligated into pET20 (Novagen) digested with NdeI and XhoI and screened as described above. Plasmids are listed in Table 1.

Purification of FBP

Cultures (10 ml) of DM9297 containing an *fbp*-expression plasmid (Table 1), grown overnight in LB with 11 mM glucose, chloramphenicol, and ampicillin, were used to inoculate 1 liter of LB with 2.5 mM glucose, chloramphenicol, and ampicillin. The culture was grown at 37 °C with shaking (200 rpm) to an optical density at 650 nm of 0.6–0.7 and induced with 1 mM arabinose. After 3 h at 37 °C, cells were harvested by centrifugation (7000 × *g*, 15 min, 4 °C). Cell pellets were resuspended in 15 ml of buffer A (50 mM sodium phosphate, 300 mM NaCl, 50 mM imidazole, pH 7.0) containing protease inhibitor mixture (Sigma P-8849) and disrupted with a French pressure cell (15,000 lb/inch^2). The crude extract was clarified by centrifugation (39,000 × *g*, for 30 min at 4 °C). The clarified extract was loaded onto a HisTrap FF column (Amersham Biosciences) equilibrated with buffer A, then the column was washed with 15 column volumes of buffer A. Protein was eluted with a linear gradient (20 column volumes) from 50 to 500 mM imidazole in buffer A. Fractions containing FBP as judged by SDS-PAGE analysis were pooled, concentrated to 7–10 mg/ml, exchanged into buffer B (10 mM potassium phosphate, 20% glycerol, 1 mM EDTA, 1 mM dithiothreitol, 0.4 mM fructose 1,6-bisphosphate, pH 7.0), frozen in liquid N_2, and stored at −80 °C.

Assay of FBP Activity

FBP activity was determined using a coupled, spectrophotometric assay (37). Aliquots of FBP were thawed and diluted to 0.05 μg/ml in buffer C (10 mM potassium phosphate, 20% glycerol, pH 7.0) immediately prior to assay. Reactions (1 ml) contained: 100 mM Tris-Cl, pH 7.5, 0–100 μM Fru-1,6-P, 0–25 mM $MgCl_2$, 2 mM ammonium sulfate, 0.2 mM $NADP^+$, 50 μM EDTA, 5 mM β-mercaptoethanol, 0.8 units of glucose-6-phosphate dehydrogenase, 0.8 units of phosphoglucose isomerase, and FBP. Reactions were initiated by the addition of FBP (250 ng), and the reduction of $NADP^+$ was monitored at 340 nm ($\epsilon = 6.22\ mM^{-1}\ cm^{-1}$). The linear steady-state portion of the A_{340} *versus* time plot was used to determine the kinetic parameters k_{cat}, K_m (Fru-1,6-P), and Hill coefficient by fitting initial velocity data to Equation 1 ($R^2 \geq 0.99$),

$$v = V_{max} \times S^H/(K_m{}^H + S^H) \qquad \text{(Eq. 1)}$$

where v is velocity, S is either the concentration of varied cofactor or substrate, V_{max} is the velocity at saturating substrate and cofactor, K_m is the Michaelis constant for the varied cofactor or substrate, and H is the Hill coefficient. The velocity data as plotted in the double-reciprocal form was fit by the following function,

$$y = (a + bx + cx^2)/(1 + ex) \qquad \text{(Eq. 2)}$$

where x is 1/[substrate], and y is 1/velocity. The initial slope is defined as $b - ae$, the slope of the asymptote is c/e, the y intercept is a, and the asymptote intercept is $(be - c)/e^2$.

TABLE 2
Mutations in *fbp* allow *purH* mutants to grow on minimal glycerol medium in the absence of histidine

Strain	Relevant genotype	FBP protein variant	Doubling time[a] (min)			
			Glucose adenine B1	Glucose adenine B1 histidine	Glycerol adenine B1	Glycerol adenine B1 histidine
DM7596	*purH355*	WT	73 ± 10	74 ± 2	NG[b]	70 ± 4
DM7597		WT	71 ± 3	76 ± 2	64 ± 5	68 ± 3
DM7833	*fbp-21*::MudJ	Null	62 ± 6	61 ± 1	NG	NG
DM8807	*purH355 fbp-22*	T19I	63 ± 2	58 ± 4	80 ± 17	78 ± 7
DM8808	*purH355*	WT	67 ± 6	62 ± 7	NG	84 ± 6
DM8809	*purH355 fbp-23*	G20D	60 ± 6	60 ± 9	94 ± 10	78 ± 11
DM8810	*purH355*	WT	68 ± 10	65 ± 7	NG	80 ± 6
DM8811	*purH355 fbp-24*	T23I	87 ± 3	64 ± 9	92 ± 3	73 ± 7
DM8812	*purH355*	WT	56 ± 2	71 ± 9	NG	77 ± 4

[a] Doubling times are calculated from the results of three independent cultures ± S.D.
[b] NG, the optical density did not increase during the course of the experiment.

Inhibition by AMP was studied by using saturating Fru-1,6-P (100 μM), five concentrations of $MgCl_2$ (0.5–8 mM), and five concentrations of AMP (0–8 μM for FBP(wt), 0–0.6 mM for FBP(T19I), and 0–8 mM for FBP(G20D) and FBP(T23I)). Inhibition by AICAR was studied by using saturating Fru-1,6-P (100 μM), five concentrations of $MgCl_2$ (0.5–8 mM), and five concentrations of AICAR (0–120 μM for FBP(wt) and 0–10 mM for mutant FBP enzymes). Inhibition data were fit to the following equation (Equation 3) for nonlinear mixed-type inhibition ($R^2 \geq 0.95$),

$$\nu = V_{max} \times S^H / [((1 + (I/K_{ic})) \times K_a) + (1 + (I/K_{iu})) \times S^H] \quad \text{(Eq. 3)}$$

where ν is the velocity, V_{max} is the velocity with saturating substrate and cofactor with no inhibitor present, K_a is the Michaelis constant for Mg^{2+}, S is the concentration of Mg^{2+}, K_{ic} is the competitive dissociation constant for inhibitor from the enzyme-inhibitor complex, K_{iu} is the uncompetitive dissociation constant for inhibitor from the enzyme-inhibitor complex, I is the concentration of inhibitor, and H is the Hill coefficient for Mg^{2+} derived from Equation 1. Linear and nonlinear regression analysis was preformed using SigmaPlot 9.0 (Systat Software).

RESULTS

Salmonella purH Mutants Are Unable to Use Glycerol as a Sole Carbon and Energy Source—The observation was made that a *purH* mutant strain of *S. enterica* (DM2) was unable to grow on minimal medium containing glycerol as sole carbon and energy source and supplemented with adenine and thiamine (Table 2). Further experiments demonstrated that this growth defect was eliminated by the addition of exogenous histidine. This finding led to the hypothesis that the accumulation of the purine biosynthetic intermediate, AICAR, was inhibiting an enzyme(s) required for growth on glycerol medium. AICAR is also generated as a byproduct of histidine biosynthesis; therefore addition of exogenous histidine reduces the intracellular concentration of AICAR in a *purH* mutant (5).

Mutations That Allow a purH Mutant to Grow on Glycerol Medium in the Absence of Histidine Map to the fbp Locus—A *purH* mutant (DM2) was plated on minimal glycerol medium supplemented with adenine and thiamine and mutagenized with diethyl sulfate (3 μl spotted in the middle of a plate containing 10^8 colony forming units). Colonies appeared within 48 h and were concentrated in a ring around the spot of diethyl sulfate; 24 colonies were purified and re-tested for the glycerol-positive phenotype. One of these mutants was a *purH*$^+$ revertant; and it was discarded. Twelve of the remaining strains were chosen at random for further study. The causative mutation in each was found to be genetically linked to a transposon located near the *fbp* locus. Six of these mutants were reconstructed and the *fbp* gene was amplified by PCR, cloned into pSU19, and sequenced. Three unique mutations were identified, causing the following amino acid substitutions: T19I, G20D, and T23I. Mutations causing the T19I and T23I substitutions were independently isolated multiple times. Isogenic strains containing each of the three mutations on the chromosome were constructed and tested for their ability to grow on minimal glycerol medium supplemented with adenine and thiamine (Table 2). The presence of any of these three mutations allowed a *purH* mutant to grow on minimal glycerol medium supplemented with adenine and thiamine. Strains containing null mutations in *fbp* also fail to grow on other gluconeogenic carbon sources such as acetate and succinate (19). In addition to glycerol, *purH* mutants failed to use acetate and succinate as sole carbon and energy sources in the absence of exogenous histidine (data not shown).

The Mutant FBP Enzymes Are Resistant to Inhibition by AICAR and AMP in Vitro—Wild-type and mutant FBP enzymes were purified as His_6-tagged fusion proteins via Ni^{2+} affinity chromatography. The purified enzymes were judged to be ~90% pure by image analysis (Phoretix TotalLab) (Fig. 2). Kinetic parameters were determined from initial velocity data for the purified enzymes as described under "Experimental Procedures." Fig. 3 shows the ν *versus* substrate concentration for varying [Fru-1,6-P] (A.1) and [$MgCl_2$](B.1) and the respective double reciprocal plots (A.2,B.2). These data as illustrated in the ν *versus* [Fru-1,6-P] and ν *versus* [Mg^{2+}] plots are best fit by a modified Hill equation and the double reciprocal plots show data that are nonlinear and have a rising trend. This is characteristic of enzymes displaying positive cooperativity. To verify positive cooperativity, Hill plots were constructed for the assays with saturating Mg^{2+} and varied Fru-1,6-P (A.3) and the assays with saturating Fru-1,6-P and varied Mg^{2+} (B.3). Both plots are linear with a slope (n) corresponding to the Hill coefficient (H) derived from Equation 1. The kinetic parameters for the wild-type and variant *S. enterica* enzymes were derived using Equation 1 and are listed in Table 3. The values obtained for the

wild-type enzyme were similar to those reported for the *E. coli* enzyme (20).

Inhibition by AMP and AICAR was examined for the wild-type and variant enzymes. The double-reciprocal plots of the v *versus* $[Mg^{2+}]$ were found to be nonlinear and inhibition visually appeared to be competitive relative to $[Mg^{2+}]$. The plots were nonlinear because of the cooperative behavior of Mg^{2+} binding to the enzymes. Linearity was obtained by raising the $[Mg^{2+}]$ to the power of the Hill coefficient of the specific enzymes, which was determined using Equation 1 (Table 3). A representative double reciprocal plot of wild-type FBP inhibition by AICAR is shown in Fig. 4. The type of inhibition exhibited for AMP and AICAR was determined by graphing initial rate data in the form of double reciprocal plots at various inhibitor concentrations and Dixon plots ($1/v$ *versus* [I]). By comparing actual data to theoretical values obtained by fitting the nonlinear data to various inhibition equations it was found that the data are best described by Equation 3 for mixed-type inhibition. The inhibition constants are shown in Table 4. This means that AMP and AICAR bind to both the E and E·Mg complex. The high K_{iu} values and low K_{ic} values obtained from the fits indicated that AMP and AICAR bind more tightly to the free enzyme and weaker to the E·Mg complex. Shown in the *inset* of Fig. 4 is a replot of the slopes for the theoretical data in Fig. 4 *versus* $[AICAR]^1$. The relationship is linear indicating that AICAR and AMP (data not shown) do not inhibit the enzymes in a cooperative manner. As predicted from the phenotypic data, all three mutant forms of FBP had significantly higher K_i values than the wild-type enzyme (K_{ic} ~ 120–1100-fold for AMP, ~45–60-fold for AICAR; K_{iu} ~ 100–1500-fold for AMP, 20–40-fold for AICAR).

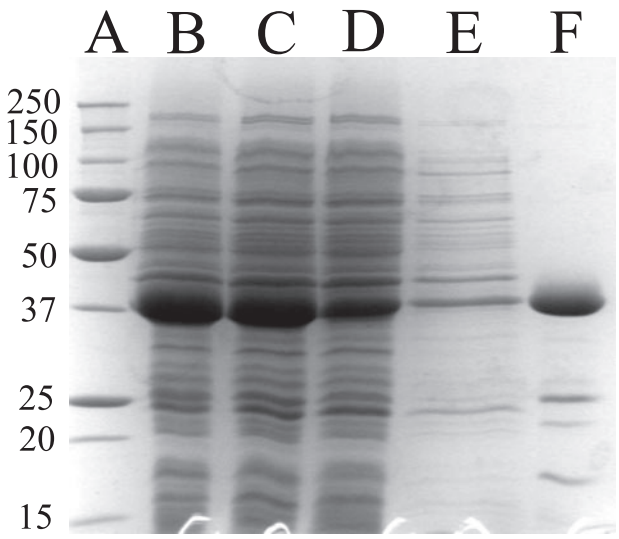

FIGURE 2. **Purification of wild-type FBP-His$_6$ using a HisTrap FF column.** *Lane A*, molecular weight marker; *lane B*, crude extract; *lane C*, clarified crude extract; *lane D*, flow-through; *lane E*, wash; *lane F*, elution.

DISCUSSION

Results herein showed that the inability of *S. enterica purH* mutants to grow on gluconeogenic carbon sources in the absence of exogenous histidine is due to inhibition of FBP by the accumulation of the purine biosynthetic intermediate AICAR. Revertant mutations restoring growth of the *purH* mutant on glycerol mapped to *fbp*, and resulted in variants of FBP that were resistant to inhibition by AICAR and AMP.

The three variant proteins characterized in this work (T19I, G20D, and T23I) had lesions located in the AMP binding site of the FBP protein as determined from the crystal structure of the pig kidney enzyme (17). As shown in the partial alignment in Fig. 5, the AMP binding site is highly conserved between both bacterial and mammalian enzymes. *S. enterica* FBP is 97% identical and 98% similar to *E. coli*

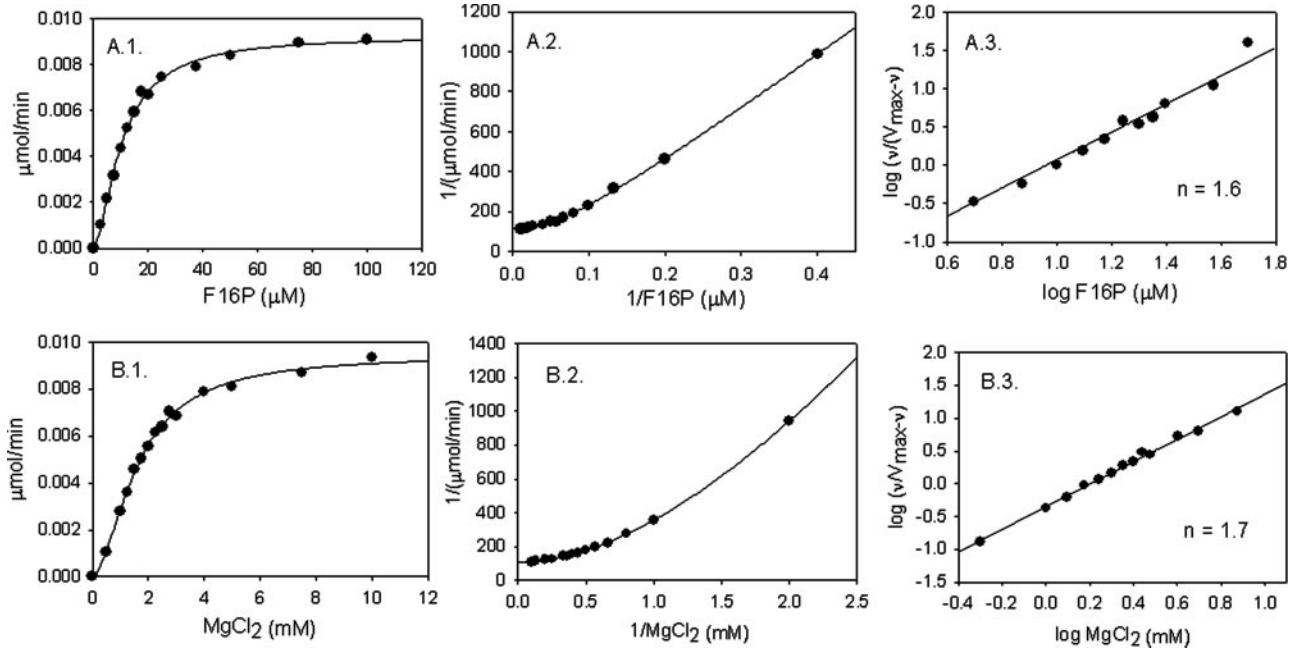

FIGURE 3. **Kinetic results demonstrate cooperative behavior for *Salmonella* FBP when Mg^{2+} and Fru-1,6-P are varied.** The plots comparing the velocity of $NADP^+$ reduction while varying the concentration of Fru-1,6-P (*series A*) or Mg^{2+} (*series B*) are shown. Plots are as follows: *1*, v *versus* [substrate or cofactor] fit by Equation 1; *2*, double reciprocal plot of 1 fit by Equation 2; *3*, Hill Plot fit using a linear regression (n = slope).

FBP, 43% identical and 63% similar to the pig kidney enzyme, and 44% identical and 63% similar to the human liver enzyme. Like the mammalian enzyme, but unlike the *E. coli* enzyme, FBP from *S. enterica* displayed cooperative kinetic behavior that had not been reported (mammalian $h_{Mg(II)} \sim 2$ (38)) (20). Interestingly, *S. enterica* FBP also displayed cooperative behavior for Fru-1,6-P that has not been reported for any FBP studied to date. Moreover, the *S. enterica* enzyme did not show cooperative kinetic behavior for AMP or AICAR inhibition, whereas this behavior has been shown for these inhibitors in the mammalian enzyme (mammalian $h_{AMP} = 2$ (16, 38, 39)).

Thr[19] corresponds to Thr[27] in the mammalian enzymes; the side chain of this residue contacts the phosphate group of AMP in the crystal structure (17), and replacement of Thr[27] in the porcine enzyme with alanine increased the K_i for AMP 1300-fold (40). In this work, the T19I substitution increased the K_{ic} for AMP 118-fold and the K_{iu} 98-fold. Thr[23] corresponds to Thr[31] in the mammalian enzymes; the side chain of this residue forms a hydrogen bond with the purine base of AMP in the crystal structure, and site-directed mutagenesis studies have confirmed its importance in AMP inhibition (39, 41). Gly[20] corresponds to Gly[28] of the mammalian enzymes, which forms a hydrogen bond to a water molecule in the AMP binding site but has not been studied by site-directed mutagenesis (42). Additional residues known to be important in AMP inhibition of the mammalian enzymes include Arg[22], Ala[24], Glu[29], Ala[54], Lys[112], Tyr[113], Gly[122], and Arg[140] (39–41, 43–45). A previous report on an AMP-insensitive *fbp* mutant of *E. coli* found that growth was unaffected by the presence of this mutation unless the allele was highly expressed, but further characterization of the enzyme was not reported (46).

The purine biosynthetic intermediate AICAR was shown to bind to the AMP binding pocket of human liver FBP by crystallographic studies (42) and shown to inhibit FBP in rat liver extracts (10, 11). All three substitutions described in this work significantly reduce inhibition of the enzyme for both AMP and AICAR. It is interesting to note that a perfect correlation does not exist between the effects of each substitution on inhibition by AMP and AICAR despite the fact that both compounds bind at the same site. In particular, the T23I substitution increases the K_{ic} for AMP 1100-fold, but only increases the K_{ic} for AICAR 31-fold. This observation may be explained by crystallographic data demonstrating that AICAR binds in a slightly different orientation than AMP; specifically, the imidazole ring of AICAR is rotated 180° relative to AMP in the crystal structure (42). The side chain of this residue forms hydrogen bonds to the

TABLE 3

Kinetic parameters for wild-type and mutant FBP enzymes

Parameters are defined under "Experimental Procedures."

Enzyme	k_{cat}	$K_m^{Fru\text{-}1,6\text{-}P}$	Hill coefficient	
			Fru-1,6-P	Mg^{2+}
	s^{-1}	μM		
FBP(wt)	24.3 ± 0.1	10.8 ± 0.4	1.59 ± 0.09	1.75 ± 0.13
FBP(T19I)	26.8 ± 0.7	9.5 ± 0.4	1.70 ± 0.12	1.65 ± 0.11
FBP(G20D)	15.0 ± 1.2	20.1 ± 3.9	1.17 ± 0.18	1.76 ± 0.20
FBP(T23I)	20.4 ± 0.7	8.5 ± 1.1	1.41 ± 0.25	1.37 ± 0.10

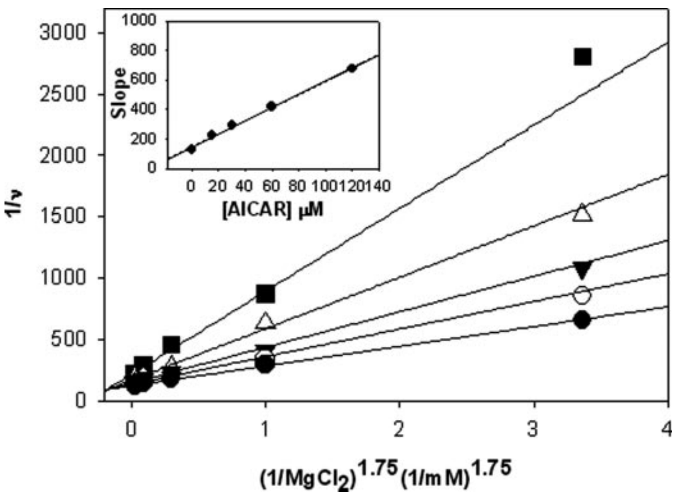

FIGURE 4. **Inhibition of wild-type *Salmonella* FBP by AICAR.** Double reciprocal plots of velocity *versus* $[Mg^{2+}]^h$ at 0 mM (●), 15 mM (○), 30 mM (▼), 60 mM (△), and 120 mM (■) AICAR. *Lines* represent plots of predicted $1/v$ *versus* $1/[Mg^{2+}]$ determined using nonlinear regression as described under "Experimental Procedures." *Inset*, replot of the slopes of the regression lines *versus* [AICAR].

TABLE 4

Inhibition constants for wild-type and mutant Fpb enzymes

Parameters are defined under "Experimental Procedures."

Enzyme	$K_a^{Mg(II)}$-AICAR[a]	K_{ic}^{AICAR}	K_{iu}^{AICAR}	$K_a^{Mg(II)}$-AMP[a]	K_{ic}^{AMP}	K_{iu}^{AMP}
	mM	μM	μM	mM	μM	μM
FBP(wt)	1.3 ± 0.1	37.3 ± 5.6	165 ± 15	2.3 ± 0.2	1.31 ± 0.26	4.14 ± 0.44
FBP(T19I)	2.7 ± 0.3	1700 ± 390	6320 ± 920	2.2 ± 0.3	155 ± 52	404 ± 53
FBP(G20D)	4.4 ± 0.5	2160 ± 510	4610 ± 750	4.6 ± 0.7	1360 ± 340	657 ± 150
FBP(T23I)	1.2 ± 0.1	1160 ± 220	3800 ± 320	2.7 ± 0.3	1450 ± 330	6120 ± 1100

[a] K_a for Mg^{2+} determined when varying either AICAR or AMP.

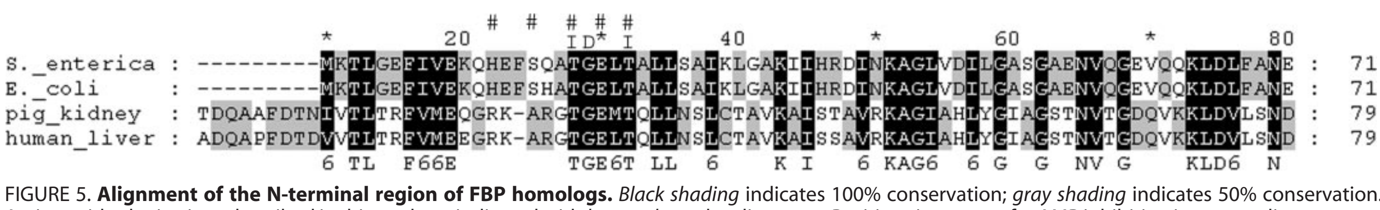

FIGURE 5. **Alignment of the N-terminal region of FBP homologs.** *Black shading* indicates 100% conservation; *gray shading* indicates 50% conservation. Amino acid substitutions described in this work are indicated with *letters above* the alignment. Positions important for AMP inhibition in mammalian enzymes are indicated by *pound signs*. *Asterisks* mark every 20 amino acids, and the *number 6* indicates conservation of a branched chain amino acid or methionine at that position. The figure was prepared with ClustalX (49) and GeneDoc (50).

purine ring and a water molecule in the AMP-bound structure, but in the AICAR-bound structure, the side chain hydrogen bond to the water molecule is replaced by a backbone nitrogen hydrogen bond from the same Thr residue. If the substitution of Ile for this Thr residue still allows the backbone hydrogen bond while eliminating the side chain hydrogen bond, this could explain the different effects of this substitution with respect to the two inhibitors.

The K_{ic} determined for AICAR with the wild-type enzyme (37.3 ± 5.6 μM) agrees well with the IC_{50} determined by Iversen *et al.* (42) for the human liver enzyme. This is significant because it indicates that AICAR inhibits FBP at a physiologically relevant concentration. Bochner and Ames (47) determined the intracellular concentration of AICAR in *Salmonella* to be 105 μM in minimal glucose medium, whereas Rohlman and Matthews (2) measured concentrations of 40–150 μM in *E. coli* strain W3110. AICAR has many physiological effects in various organisms. These data suggest that in enteric bacteria AICAR has the potential to affect flux through gluconeogenesis, as FBP is a key control point for this pathway. The concentration of AICAR would be expected to decrease in response to exogenous purines or histidine due to feedback inhibition of the biosynthetic pathways for these compounds. It is known that AICAR levels increase significantly in response to folate stress (~3–6-fold) due to inhibition of the PurH enzyme (1, 2). Genetic evidence suggests that the PurH enzyme is sensitive to high temperature (48). Considering the *in vitro* kinetic parameters and *in vivo* pool sizes, it seems likely that flux through gluconeogenesis may be altered under growth conditions that impact the concentration of AICAR exemplified by blocking PurH by mutation.

In summary, the work described here has identified three amino acid substitutions in FBP from *Salmonella* that cause insensitivity to both AMP and AICAR. An additional potential regulatory role for the small molecule AICAR has been identified, although further work is necessary to determine whether this effect is physiologically relevant. Finally, the use of *purH* mutants could provide a powerful genetic selection for AMP-insensitive mutants of FBP, including substitutions that might not be predicted based on structural information.

Acknowledgments—We acknowledge P. Frey and W. W. Cleland (Department of Biochemistry, University of Wisconsin-Madison) for advice on the kinetic analysis.

REFERENCES

1. Bochner, B. R., and Ames, B. N. (1982) *Cell* **29,** 929–937
2. Rohlman, C. E., and Matthews, R. G. (1990) *J. Bacteriol.* **172,** 7200–7210
3. Soberon, M., Lopez, O., Miranda, J., Tabche, M. L., and Morera, C. (1997) *Mol. Gen. Genet.* **254,** 665–673
4. Rebora, K., Laloo, B., and Daignan-Fornier, B. (2005) *Genetics* **170,** 61–70
5. Allen, S., Zilles, J. L., and Downs, D. M. (2002) *J. Bacteriol.* **184,** 6130–6137
6. Corton, J. M., Gillespie, J. G., Hawley, S. A., and Hardie, D. G. (1995) *Eur. J. Biochem.* **229,** 558–565
7. Kahn, B. B., Alquier, T., Carling, D., and Hardie, D. G. (2005) *Cell Metab.* **1,** 15–25
8. Xiang, X., Saha, A. K., Wen, R., Ruderman, N. B., and Luo, Z. (2004) *Biochem. Biophys. Res. Commun.* **321,** 161–167
9. Rattan, R., Giri, S., Singh, A. K., and Singh, I. (2005) *J. Biol. Chem.* **280,** 39582–39593
10. Vincent, M. F., Marangos, P. J., Gruber, H. E., and Van den Berghe, G. (1991) *Diabetes* **40,** 1259–1266
11. Vincent, M. F., Erion, M. D., Gruber, H. E., and Van den Berghe, G. (1996) *Diabetologia* **39,** 1148–1155
12. Benkovic, S. J., and deMaine, M. M. (1982) *Adv. Enzymol. Relat. Areas Mol. Biol.* **53,** 45–82
13. Tejwani, G. A. (1983) *Adv. Enzymol. Relat. Areas Mol. Biol.* **54,** 121–194
14. Pilkis, S., El-Maghrabi, M., Pilkis, J., and Claus, T. (1981) *J. Biol. Chem.* **256,** 3619–3622
15. Ke, H., Thorpe, C. M., Seaton, B. A., Lipscomb, W. N., and Marcus, F. (1990) *J. Mol. Biol.* **212,** 513–539
16. Taketa, K., and Pogell, B. M. (1965) *J. Biol. Chem.* **240,** 651–662
17. Ke, H. M., Zhang, Y. P., and Lipscomb, W. N. (1990) *Proc. Natl. Acad. Sci. U. S. A.* **87,** 5243–5247
18. Liang, J. Y., Zhang, Y., Huang, S., and Lipscomb, W. N. (1993) *Proc. Natl. Acad. Sci. U. S. A.* **90,** 2132–2136
19. Fraenkel, D. G., and Horecker, B. L. (1965) *J. Bacteriol.* **90,** 837–842
20. Kelley-Loughnane, N., Biolsi, S. A., Gibson, K. M., Lu, G., Hehir, M. J., Phelan, P., and Kantrowitz, E. R. (2002) *Biochim. Biophys. Acta* **1594,** 6–16
21. Marcus, F., Edelstein, I., and Rittenhouse, J. (1984) *Biochem. Biophys. Res. Commun.* **119,** 1103–1108
22. Hers, H. G., and Hue, L. (1983) *Annu. Rev. Biochem.* **52,** 617–653
23. Babul, J., and Guixe, V. (1983) *Arch. Biochem. Biophys.* **225,** 944–949
24. Hines, J. K., Fromm, H. J., and Honzatko, R. B. (2006) *J. Biol. Chem.* **281,** 18386–18393
25. Castilho, B. A., Olfson, P., and Casadaban, M. J. (1984) *J. Bacteriol.* **158,** 488–495
26. Way, J. C., Davis, M. A., Morisato, D., Roberts, D. E., and Kleckner, N. (1984) *Gene* (*Amst.*) **32,** 369–379
27. Davis, R. W., Botstein, D., and Roth, J. R. (1980) *Advanced Bacterial Genetics*, Cold Spring Harbor Laboratory, Cold Spring Harbor, NY
28. Vogel, H. J., and Bonner, D. M. (1956) *J. Biol. Chem.* **218,** 97–106
29. Beck, B. J., and Downs, D. M. (1998) *J. Bacteriol.* **180,** 885–891
30. Petersen, L., Enos-Berlage, J., and Downs, D. M. (1996) *Genetics* **143,** 37–44
31. Schmieger, H. (1972) *Mol. Gen. Genet.* **119,** 75–88
32. Roberts, G. P. (1978) in *Isolation and Characterization of Informational Supressors in Salmonella typhimurium.* Doctoral dissertation, University of California, Berkeley, CA
33. Downs, D. M., and Petersen, L. (1994) *J. Bacteriol.* **176,** 4858–4864
34. Kleckner, N., Roth, J., and Botstein, D. (1977) *J. Mol. Biol.* **116,** 125–159
35. Caetano-Anolles, G. (1993) *PCR Methods Appl.* **3,** 85–94
36. Webb, E., Claas, K., and Downs, D. (1998) *J. Biol. Chem.* **273,** 8946–8950
37. Pontremoli, S., Traniello, S., Luppis, B., and Wood, W. A. (1965) *J. Biol. Chem.* **240,** 3459–3463
38. Nimmo, H. G., and Tipton, K. F. (1975) *Eur. J. Biochem.* **58,** 575–585
39. Chen, M., Chen, L., and Fromm, H. J. (1994) *J. Biol. Chem.* **269,** 5554–5558
40. Shyur, L. F., Aleshin, A. E., Honzatko, R. B., and Fromm, H. J. (1996) *J. Biol. Chem.* **271,** 3005–3010
41. Gidh-Jain, M., Zhang, Y., van Poelje, P., Liang, J., Huang, S., Kim, J., Elliott, J., Erion, M., Pilkis, S., and Raafat el-Maghrabi, M. (1994) *J. Biol. Chem.* **269,** 27732–27738
42. Iversen, L. F., Brzozowski, M., Hastrup, S., Hubbard, R., Kastrup, J. S., Larsen, I. K., Naerum, L., Norskov-Lauridsen, L., Rasmussen, P. B., Thim, L., Wiberg, F. C., and Lundgren, K. (1997) *Protein Sci.* **6,** 971–982
43. Zhang, R., Chen, L., Villeret, V., and Fromm, H. J. (1995) *J. Biol. Chem.* **270,** 54–58
44. Kelley-Loughnane, N., and Kantrowitz, E. R. (2001) *Biochim. Biophys. Acta* **1548,** 66–71
45. Iancu, C. V., Mukund, S., Fromm, H. J., and Honzatko, R. B. (2005) *J. Biol. Chem.* **280,** 19737–19745

46. Sedivy, J. M., Babul, J., and Fraenkel, D. G. (1986) *Proc. Natl. Acad. Sci. U. S. A.* **83,** 1656–1659
47. Bochner, B. R., and Ames, B. N. (1982) *J. Biol. Chem.* **257,** 9759–9769
48. Downs, D. M. (1987) in *Purine Metabolism and Cryptic Prophages in Salmonella typhimurium.* Doctoral dissertation, University of Utah, Salt Lake City, UT
49. Thompson, J. D., Gibson, T. J., Plewniak, F., Jeanmougin, F., and Higgins, D. G. (1997) *Nucleic Acids Res.* **25,** 4876–4882
50. Nicholas, K. B., Nicholas, H. B., Jr., and Deerfield, D. W., II. (1997) *EMBnet News* **4,** 14
51. McKinney, J., Guerrier-Takada, C., Galan, J., and Altman, S. (2002) *J. Bacteriol.* **184,** 6056–6059
52. Bartolome, B., Jubete, Y., Martinez, E., and de la Cruz, F. (1991) *Gene* (*Amst.*) **102,** 75–78
53. Chang, A. C., and Cohen, S. N. (1978) *J. Bacteriol.* **134,** 1141–1156
54. Studier, F. W. (1991) *J. Mol. Biol.* **219,** 37–44